Full-scale Field Test Extraction of Natural Frequency and Acceleration of Bridge using Modal Test and Operational Modal Analysis

Wan Ikram Wajdee Wan Ahmad Kamal[1], Izni Syahrizal Ibrahim[2], Khairul Hazman Padil[2], Sarehati Umar[1], Han-Seung Lee[3] and Jitendra Kumar Singh[3]

[1]School of Civil Engineering, Faculty of Engineering, Universiti Teknologi Malaysia, 81310 Johor Bahru, Johor, Malaysia
[2] Forensic Engineering, Centre, Institute of Smart Infrastructure and Innovative Construction, School of Civil Engineering, Faculty of Engineering, Universiti Teknologi Malaysia, 81310 Johor Bahru, Johor, Malaysia
[3] Innovative Durable Building and Infrastructure Research Center, Hanyang University, Ansan, South Korea

Corresponding author's e-mail: wanikramwajdee@utm.my

Abstract. Vibration in bridges occurred due to several factors such as structural design, environmental loadings, and loading characteristics (speed parameter, loading patterns, and configuration of axles). If this problem is prolonged for several years, this may lead to stages of failure such as structural cracking, fatigue on structural members, excessive deformation, and local stress concentration on structural connections. In response to this issue, an investigation was carried out in this study by utilising numerical modelling of Finite Element Analysis (FEA) to explore the effect of the Intermediate Diaphragm (ID) on the RC bridge deck. The FEA is then validated and confirmed from the full-scale field-test, which consists of a modal test for both frequency and mode shape comparisons, and operational modal analysis for extraction of deck acceleration. The results show that the current natural frequency of the bridge does not reach the minimum frequency requirement from the BS5400 Code of Practice, while the acceleration based on a 24-tonnes moving truck is within the allowable acceleration limit. In comparison, frequency, mode shape and acceleration between the FEA numerical analysis and field test had shown insignificant differences and minimum error between the two.

1.0 Introduction

In general, the vibration of structure is not a new phenomenon to any type of structure carrying its intended load bridge structures in particular, which carry transient or moving loads. According to the structural dynamic principle, whenever a structure such as a bridge is imposed to a dynamic or moving load where the frequency loading is much higher than the natural frequency, a vibration phenomenon would take place in turn structure becomes wavered by itself for seconds. This case is sometimes known as resonance. Resonance can usually be felt due to the effect of road users or pedestrians passing by the affected bridge. The vibration of the affected structure can be seen to behave known as a 'dancing act' if the difference between the loading frequency and natural vibration is so high. Several cases had been

reported due to the implication of vibration on the bridge which, could jeopardize the riding quality of the bridge users [1], [2]. Somehow if this vibration event was continuously triggered without any remedial care, it can lead to the failure of the bridge and in the worst-case scenario, the collapse of the bridge when a catastrophic level was reached [1], [3]. Moreover, a bridge that experienced continuous vibration is expected to suffer from fatigue which makes the bridge remain in excessive deformation. This run-down could result in an out-of-capacity structure in terms of its elastic capacity to resist the applied load [4], [5]. It had been previously studied and documented that vibration can displace the elastomeric rubber bearing from its intended location. This had occurred in many cases for the beam-to-slab bridges [6]–[8]. This information is good enough to increase awareness among designers that the vibration issue is very significant and needs to be controlled to minimize catastrophic failures in the future. In addition, this specific vibration case can result in distortion on some of the bridge components such as the pier and deck slab. From here, this may continue to other attached auxiliary components on the bridge structure to detach away from its location such as rail steel, expansion joint and road signage [8]–[10]. Vibration on the beam-to-slab bridge may also result in the occurrence of local stresses on the bridge girders, especially when they are exposed to wheel loads, thus creating undesirable noise from the expansion joints[3], [6], [7], [9]. Furthermore, in the long run, the bridge could have resulted in structural cracking, thus, reducing the stiffness of the structure. This reduction in stiffness can affect the behaviour of the structure in both the frequency and mode shape in the event of dynamic load [11].

1.1. Objectives

The study is to evaluate the current vibration level and checked whether it had impaired the serviceability of the existing reinforced concrete (RC) bridge due to the daily traffic loading. The output, which is expected to be extracted from the field test is vertical acceleration, the natural frequency of the RC bridge, and mode shapes. The field test was performed on one-span RC bridge only since the superstructure consisted of a simply supported condition. There were two (2) dynamic tests performed in this experiment. The first test consists of ambient vibration or modal testing to acquire the natural frequency of the RC bridge and its mode shapes. Meanwhile, the second test consists of the operational modal analysis (OMA) or force vibration test which is to measure the acceleration of the structure as a result of the applied imposed or vehicle load.

1.2. Bridge descriptions

The entire length of the highway project is approximately 3 km consisting of four (4) numbers of slips-roads. Along the highway stretch, there is one (1) specific area where a RC bridge was required to support the road alignment. This bridge was designed to support two (2) routes which are slip road 2 and slip road 3 as shown in Figure 1.

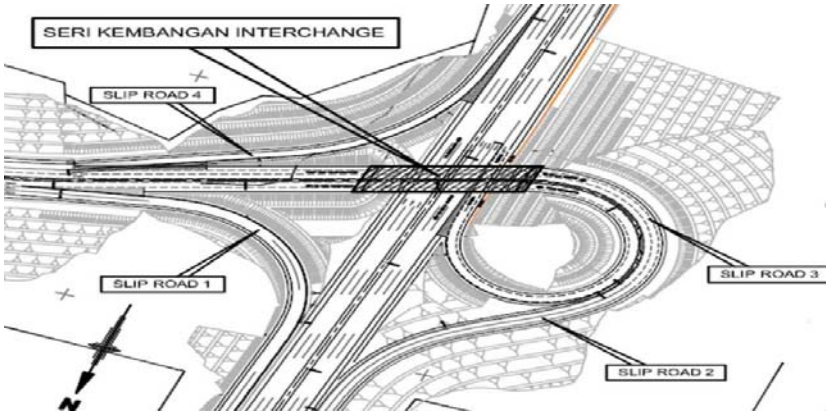

Figure 1. Key plan of the RC bridge.

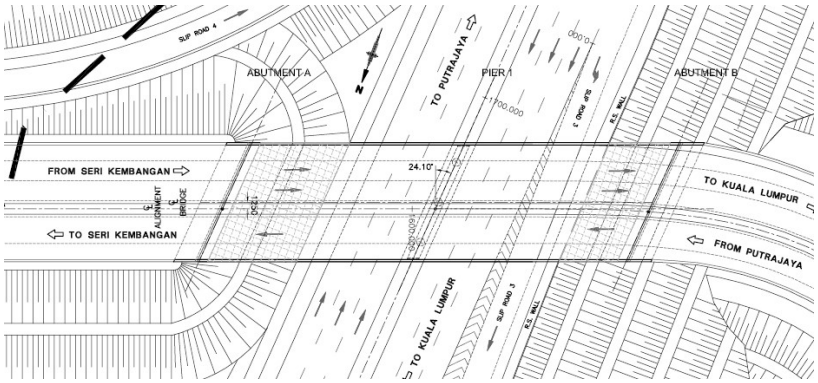

Figure 2. The RC bridge is in aerial view.

The RC bridge featured 2 spans of 40 m in length each as shown in Figure 2. The decking components comprised of 10 numbers of post-tensioned precast T-beams of 2.150 m depth for each span, 180 mm thick in-situ RC slab and spaced approximately at 2.2 m between the beams horizontally, thus owing to a 22.4 m carriageway width. The articulation system for this RC bridge is a simply supported system with a link slab running over the intermediate pier. The following figures (see Figure 3 : General arrangement of 2-span simply supported RC bridge consisting of 40 m prestresses concrete girders, Figure 4 : Cross Section of RC bridge with consisting of 10 Nos girders for 22.60 m carriageway width, and Figure 5 : Underneath bridge view showing the intermediate pier which situated at median mainline) shown the bridge features.

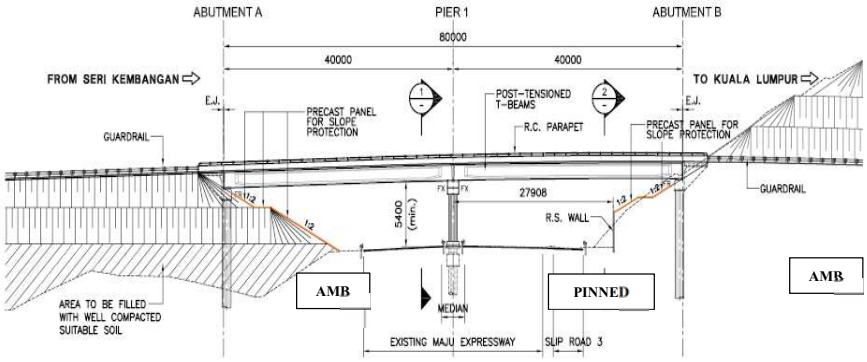

Figure 3. Elevation of span configuration of the RC bridge.

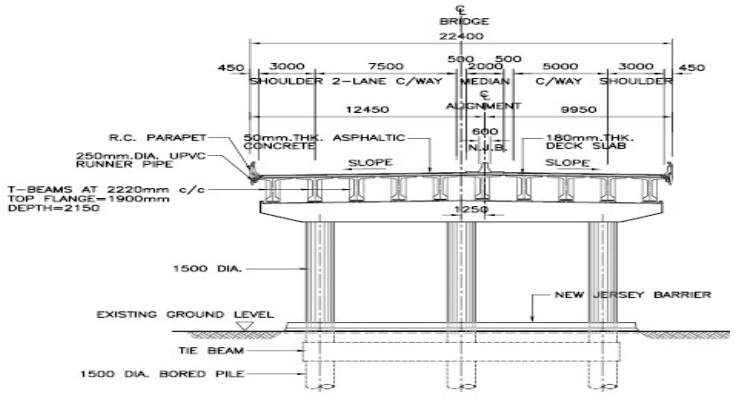

Figure 4. Typical pier cross-section.

Figure 5. Aerial view of the RC bridge.

2. Introduction to the full-scale test

Since the late 19th century, bridges had been subjected to dynamic field testing. Many of the previous studies [12]–[16] involved measuring the bridge vibrations as part of a safety check (especially on railway bridges). Modern test methods are advanced refinements of these earlier investigations [17]. Full-scale dynamic testing is performed for a variety of reasons which includes:

1. Dynamic assessments of a full-scale test enabled the creation of a database of similar dynamic behaviour on the structure.
2. Verification of conceptual model structure. Significant assumptions are made in mathematical models of real structures, especially when it comes to boundary conditions. The structure can be better understood by comparing and correlating theoretical predictions with a measured response.
3. As controls and procedures to confirm that a system's behaviour matches expectations. This gives essential data for future designs while also providing performance information on the completed structure.

Structures can benefit from full-scale dynamic testing to understand how they performed and behaved in service. Modal parameters (natural frequencies, mode shapes, and modal damping) and system parameters (stiffness, mass, and damping matrices) can be calculated from the recorded dynamic response generated by ambient or forced stimulation. These parameters can then be used to characterise and monitor the performance of the structure [17].

2.1 Theoretical Background of Vibration Testing

An evaluation of the limits of a system's response is given through modal analysis. Each structure has its inherent frequency (also known as a resonant frequency) at which it can vibrate [18]. The resonance frequency is the frequency at which an object will permit an energy transfer from one form to another with the least amount of loss. Every vibratory system has a way to store potential energy (in the form of a spring or elastic property), a method to store kinetic energy (in the form of mass or inertia), and a way to gradually release energy (damper) [18], [19]. There are four distinct classifications for vibration: (1) Forced and free/ambient vibration. (2) Damped and Un-damped vibration. (3) Nonlinear and linear vibration. (4) Random and predictable vibration. Nonlinear problems account for the majority of actual issues. Excitations (inputs) and responses (outputs) are two dynamic variables in a vibratory system that are time-dependent. Computational mathematics, governing equation formulation, equation solution, and result interpretation are all part of the analysis of a vibrating system. Vibration analysis is the technique of determining a system's or structure's frequency and using that indicators to evaluate the system's and its related components' overall health [18]–[20] Vibration analysis can identify issues like natural frequencies, resonance, structural defects and imbalanced structural system. Three key parameters are identified by all vibration analysis techniques namely : (1) Acceleration: very crucial information in high frequency, (2) Displacement or Amplitude : It is classified as important on low frequency, and (3) Velocity : very useful for both high and low frequencies. Four domains provide detailed information on how vibrating parts operate : (1) Time Domain : The signal that vibrates is the time domain which is amplitude against time, (2) Frequency Domain : The signal is shown as frequency vs. amplitude in the frequency domain, (3) Joint Domain : When vibration signals fluctuate over time, the signal can be useful in calculating various spectra at once. This is accomplished using the Joint domain, and (4) Modal Analysis : carried out to discover vibrational modes. By altering mass and stiffness, the model is evaluated. Natural frequencies and mode shapes are products of boundary conditions and structural characteristics. Natural frequencies change as structural qualities change, however mode shapes may not always automatically change. Both the natural frequency and the mode forms vary when the boundary conditions change. The Fourier transform breaks down a time function (signal) into the constituent frequencies, meanwhile the inverse Fourier transform integrates contributions from various frequencies to reproduce the original time function.

2.2 Relationship between Frequency Response Function (FRF) and the Transfer Function (TF)

Global dynamic properties (natural frequency, damping, and mode shape) can be measured for its integrity assessment using vibration testing and modal analysis. Accelerometers or other response transducers are commonly used in vibration testing, to determine the reaction of the structure. This is also to artificially creates excitation forces or ambient forces in the service environment. [19]. The transfer function is a mathematical model describing a physical system's input-output relationship. Excitation of the system resulted in a reaction (input or output). The frequency response of the system is dictated by the motion equation when excitement is applied. The transfer function is described mathematically as the output of the Laplace transform divided by the input of the Laplace transform. The frequency response function on the other hand is related to the transfer function and is defined identically. The frequency response function is represented mathematically as the output of the Fourier transform divided by the input of the Fourier transform. These expressions are frequently used interchangeably and can lead to confusion. The FRFs were determined by dividing the output accelerometer of the Discrete Fourier Transform (DFT) against the input load input of the DFT. The data quality was then evaluated using the coherence function. The modal testing technique can help to understand this relationship even more. Frequency response functions are the measurements taken during a modal test. The parameter estimation procedures are, in general, Laplace domain curve fits which yield transfer functions [19], [21].

2.2.1 System Assumption. Two major assumptions underpinned both the structural dynamics background theory and the modal parameter estimation theory, which are uniformly and at stationary. There are a few other system assumptions to consider, such as observability, stability, and practical realizability[21]. These assumptions, on the other hand, are frequently addressed in the intrinsic features of mechanical systems. As a result, unlike the assumptions of linearity and stationarity, they do not impose potential limitations on the frequency response measurement.

2.3 Experiment 1: Modal Testing (Experimental Modal Analysis-EMA)

2.3.1 Instrumentation. Modal testing is recommended over modal analysis because of the ability to generate data that may be used to better identify system parameters and modal properties. Low-input energy levels can yield measurable responses (acceleration, velocity, displacement, frequency) due to dynamic amplification. The measured responses can be used to calculate dynamic system and modal parameters. This testing is also known as Experimental Modal Analysis (EMA) (shown in Figure 6a and Figure 6b). EMA used Modal Hammer (model TLD086D50) (Figure 10b) with an approximate weight is 5.5 kg acted as an impact force generator (with the sensitivity of 0.2328 mV/N), 3 units of PCB piezotronics uniaxial accelerometer (model 352C33 with the sensitivity of 10.53 mV/ms^2), fibre optic cables, dynamic acquisition DAQ- (SIRIUS-XHS) system consists of 8 channels for data processing (shown in figure 8), portable generator producing 800 watt of electrical power (shown in Figure 7a) and a hardware processor with Dewesoft software for data acquisition and analysis purpose. The accelerometers were arranged at the centre of the carriageway (near to the median barrier) as which also represents of the centreline of the RC bridge.

Figure 6a. A hitting point in progress to get bridge response in the form of frequency and mode shapes.

Figure 6b. Demarcation of excitation points and accelerometers location

Figure 7a. 800-watt portable generator for power supply

Figure 7b. Fibre optic cable for accelerometer and DAQ.

.

Figure 8. Data acquisition-DAQ (Sirius XHS) 8 channels.

2.3.2 Loading 1. In this field test experimental work, the primary load had been incorporated to excite the response of the deck. The following is a detailed description of the imposed load:

Excitation force: This load was used for EMA modal testing simulation. The weight of the hammer is approximate 5.5 kg and is used to exert the impact force on the structure. This impact force was generated by hitting the concrete deck with the modal hammer to exert the impact force on the RC bridge structure. This excitation force in turn excites the bridge deck response (as shown in Figure 9). This response was then processed based on the frequency response spectrum wave to identify the natural frequency of the RC bridge as well as the mode shapes through signal processing of electric device known as Data analyser-DAQ (as shown in Figure 8 and Figure 9).

Figure 9. Stage of loading by hammering the deck to generate the responses

2.3.3 Stage of Loading 1. Firstly, the demarcation of the boundary for the working area was made by placing the plastic barrier. Then, the 5-excitation points and 3-detection were identified and marked using white spray (at 3.0 m to 5.0 m spacing and 6.0 m and 10.0 m spacing 3-detection points), respectively as shown in Figure 11. Several accelerometers were then placed and mounted on the road surface by using double-sided acrylic tape at the selected response point. The fibre-optic wire was finally installed to the link between the impact hammer and DAQ box as well as the accelerometers and DAQ box. A portable generator was used to supply power for the DAQ box and laptop along with the Dewesoft program to be activated once the installation stage was ready. The bandwidth of 2000 sampling frequency was chosen following the hammer and accelerometer sensitivity. Each excitation point (5 points) was hammered or knocked twice. The frequency reading and coherence after each knocking/hitting were checked. The frequency reading, as well as generated mode shapes, were recorded and saved, and the information was saved in the Transfer Function format.

Figure 10a. PCB piezotronics uniaxial accelerometer (model 352C33).

Figure 10b. Modal hammer (model TLD086D50).

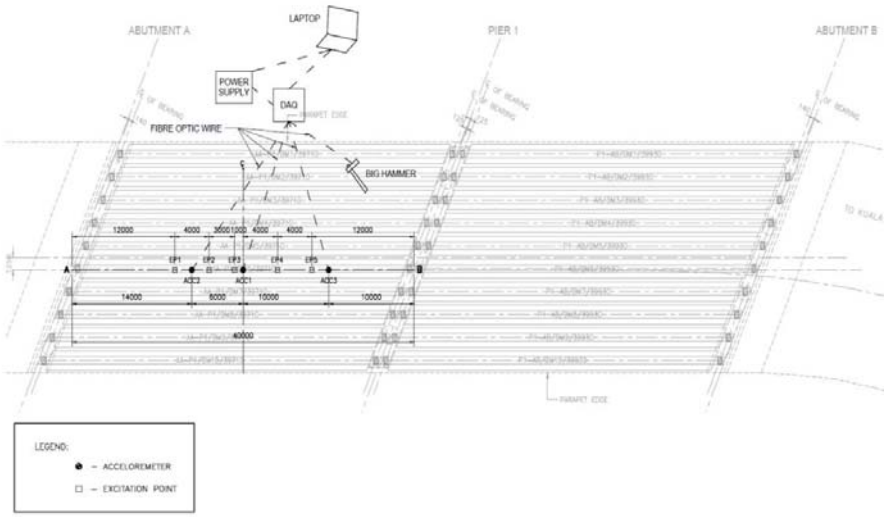

Figure 11. Ambient vibration test setup

Figure 12. Hammering points is in progress to get bridge response in term of frequency and mode shapes.

2.4. Experiment 2: Operation Modal Analysis (OMA)

2.4.1. Instrumentation. Similar to the modal test, except for the modal hammer, three (3) units of accelerometers (with the sensitivity of 10.53 mV/ms^2), fibre optic cables, a dynamic analyzer DAQ, a portable generator, and one (1) laptop with Dewesoft program for the signal reading purpose were used for OMA test. For this test, loading was applied using a 24 tonnes truck (refer to Figure 13a and Figure 13b) to simulate the vibration force. During the test, the truck was guided to move along the centre of the RC bridge deck (as shown in Figure 16 and Figure 17). The path length for the truck is 32 m based on the on-site measurement. This step was repeated three (3) times to ensure the validity of the recorded data.

Figure 13a. 24 tonnes truck with a full load of sand material moving along the 32 m path length for the OMA test.

Figure 13b. OMA test on the RC bridge deck in progress.

2.4.2. Loading 2. Meanwhile, for the OMA test, the primary load that was considered for this test is a unit of the 24-tonnes truck to excite the response of the deck. The following statement is the description for this load:

Imposed load: A moving wheels load consisting of a 3-axles (10 tyres) truck weighing 24 tonnes (Figure 14a and Figure 14b) with a full load of sand material to induce the force vibration for the OMA test. This loading configuration was chosen since its high availability on most highways in Malaysia and the spacing of the axles is considered quite close to create a high intensity of pressure load between the tyres and road due to the overlapping of the load dispersal.

Figure 14a. 24 tonnes truck with a full load of sand material in the OMA test at the weighing station for the weight measurement of the front axle.

Figure 14b. 24 tonnes truck with a full load of sand material loaded used for the OMA test at the weighing station for the weight measurement of the rear axle.

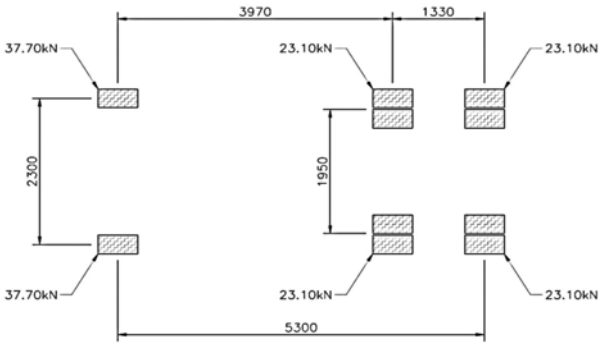

Figure 15. Truck wheels configuration for the OMA test.

2.4.3. Stage of Loading 2. Firstly, the measurement points were marked with white paint for the 3-response points according to Figure 16. The short line parallel to the new jersey barrier (NJB) with a 0.835m offset was then created as a guide for the truck movement. These short lines will guide the truck in the movement process. In addition, the start and end points for the truck were also made white painted. Next, the installation of the fibre optic wire between accelerometers and DAQ was done. The portable generator was used to power the DAQ box and the laptop with Dewesoft software. Finally, similar to the modal test, bandwidth frequency (2000Hz sampling frequency) was tuned following the accelerometer sensitivity.

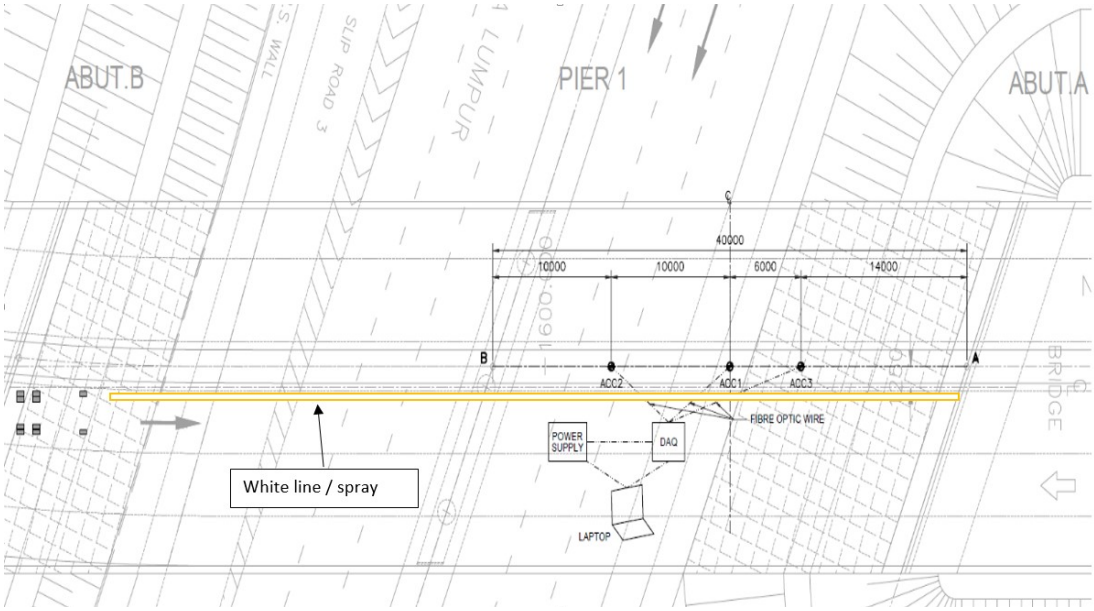

Figure 16. Equipment Setup for the OMA test.

The travel time from the start of the truck to moving until it stopped was recorded. The recorded travelling time was 9 seconds for the 32.0 m path length. The result from the OMA test in the form of vertical acceleration was recorded and analysed.

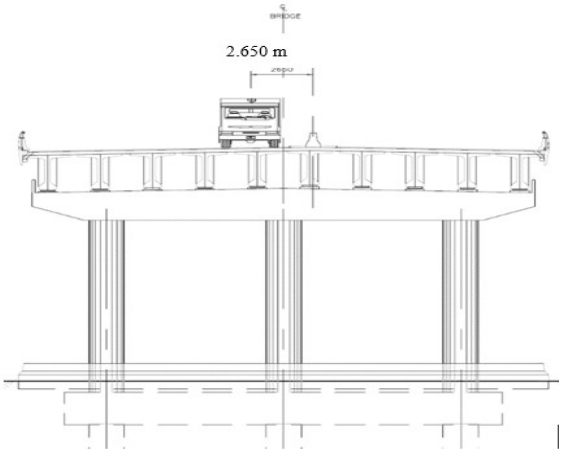

Figure 17. Arrangement for the OMA test where 2.650 m distance was defined between the centreline of the truck and road barrier.

3.0. Processing or analysing of data

3.1. Response Function Outputs. The recorded signals on-site were played again (after data collection on-site) in the office following each set of tests, and for each series, a total of 15 FRFs from 3 channels (three inputs and five outputs in the vertical direction) were computed using frequency sampling (rate), within the frequency range of 0-2000 Hz. The Discrete Fourier transform (DFT) of the accelerometer outputs were divided by the DFT of the load input, the Frequency Response Functions (FRF) were generated. To evaluate the data's quality, the coherence function was deployed. The FRFs were recorded to laptop storage (memory), and further analysis to identify the natural frequencies, mode shapes, and acceleration was carried out by using manual filtering or checking through Microsoft Excel software.

3.2. *Modal Parameter Extraction.* Natural frequencies, viscous damping ratios, and mode shapes were extracted from the response functions using a single-degree-of-freedom model. The next step was the saved or recorded FRP data exported or converted into Microsoft Excel sheet format from Dewesoft outputs to identify the natural frequencies in turn to generate the correspondence mode shapes. For the generation of mode shapes, the acceleration results of structure responses were used with the respective location (coordinates) of 5 excitation points and were then plotted for the mode shape results. Based on these plotted results and the co-existence natural frequencies, these results and the FEA results were compared in terms of acceleration, mode shapes and natural frequencies. The percentage of differences for both results (FEA and Field Test) were computed and analysed for FEA correlation if the error is more than 15% because it is considered a major error for this study.

3.3. Correlation of Finite Elements. Problems involving structural mechanics can be solved numerically using finite element analysis. In more detail, it is an analytical technique for figuring out a structure's modal characteristics. It is frequently important to confirm the outcomes of this theoretical prediction using actual data from a modal test. There are two main steps in this correlation method, which is an iterative process. First, the comparison and quantification of the discrepancies between the modal parameters, acceleration, frequencies, and mode shapes. Second, to get more similar results, alterations and adjustments are typically performed to the finite element model. As explained above (as described in section 2.1), the manipulation or adjustment of stiffness and boundary conditions are giving impact to the modal properties of the structure and therefore the common step to minimize the difference

between FEA and field test results. However, for this study, none of such action was taken place since the results difference between FEA and field test results are insignificant.

4.0 Results and verification and discussion

4.1. Frequency, Mode Shapes and Vertical Acceleration results

In general, for the modal test on-site, the displace/mode shapes of the longitudinal centerline (benchmark) of the bridge (single line) were used to compare with the median barrier element in numerical modelling. This approach was thought since the central longitudinal single line adjacent to the median barrier was a relevant element for purpose of comparison with a median barrier in modelling. Meanwhile, for acceleration results, the measurement point at the mid-span of the bridge length was the target location for the measurement of the result.

4.1.1 *Results of Experimental 1 (EMA).*

Attached below are several figures (as shown in *Figure 18a, Figure 18b, Figure 19a, Figure 19b, Figure 20a, Figure 20b, Figure 21a, Figure 21b, Figure 22a, Figure 22b, Figure 23a, Figure 23b, Figure 24a, Figure 24b, Figure 25a and Figure 25b*) that show results of frequencies coupled with respective mode shapes and vertical acceleration results of the bridge deck. These 2 experimental results were extracted for verification purposes which are needed for comparison between field test results and numerical estimation results (Abaqus results). Verification works have been made throughout these two dynamic tests *(EMA and OMA)* to confirm the accuracy of the numerical analysis results. This confirmation by experimental verification is needed to be performed to ensure that all the parameter values that were assumed *(Concrete Elasticity, Steel elasticity, strength of materials, Poisson ratio, and densities*) remained sensible as well as accurate results [22][23][24]. Generally, based on the given results both experimental and numerical results the differences in the results are not so significant. For example, the acceleration and frequency magnitudes/mode shapes (First, Second order, and Third mode) are almost identical between field results and prediction results although there are a few differences in terms of pattern shape especially mode shapes because of the disturbance from ambience /environment vibration loadings such as wind, random operational traffic load and unnecessary white noise were minimized or controlled. This action was done by closing the current operational or live traffic flow for a while (4 minutes) during the excitation of the bridge and collection of response signals or results. By imposing this control action, any unnecessary white noise and disturbance input could be hindered in turn can improve the quality of results generation (*Mode Shapes, Frequency*) [25][26]. Nevertheless, there is a minor discrepancy between both results (*Experimental* and *Numerical Analysis* results) This minor anomaly or error might happen due to several factors such as the provision of accelerometer units was not adequate for signal detection purposes (smooth shapes), the accelerometer was not mounted sufficiently on the road surface/deck, ambient vibration due to low wind speed, and probably there was some disturbance from personnel movement in the vicinity of site measurement [27][28][29]. These factors are possibilities contributing that influenced and affected the result values on site. The rhythm of data results is also different. This difference could be the variation of material properties from the actual bridge structure that changes over time due to time-dependent effects such as concrete creep coefficient, modulus elasticity value, and shrinkage strain value. These factors are attributed to giving an impact on the performance of the bridge structure which affects to data collection comparison between both methods (*Field Test and Numerical Analysis),* especially in terms of the natural frequency of structure as well as structural deformation (*mode shapes*).

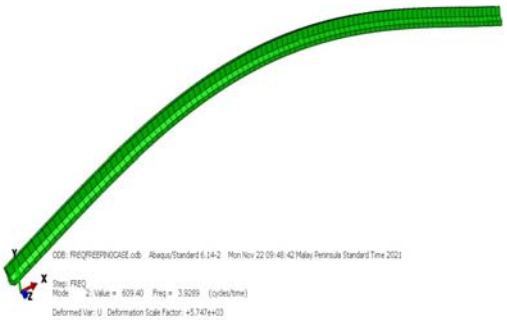

Figure 18a. First Bending Mode shape (3.929 Hz) based on numerical analysis (Abaqus).

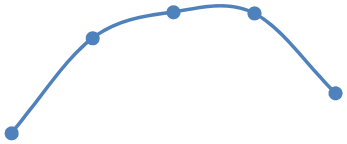

Figure 18b. First Bending Mode shape (3.921 Hz) based on Modal Testing (Experimental).

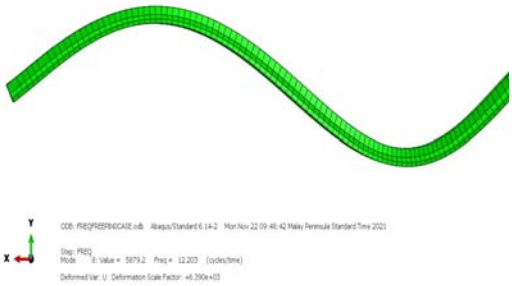

Figure 19a. Second Bending Mode (2nd Order) shape (12.203 Hz) based on numerical analysis (Abaqus).

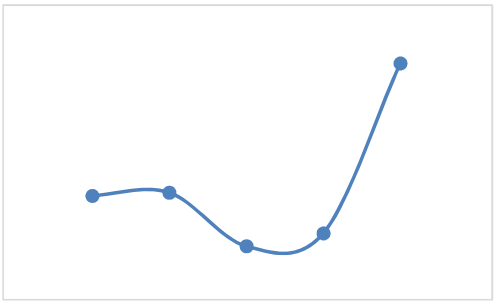

Figure 19b. Second Bending Mode (2nd Order) shape (12.207 Hz) based on modal testing (Experimental).

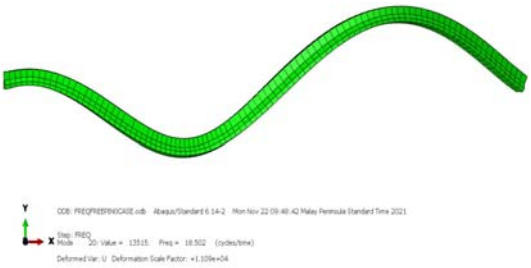

Figure 20a. Third Mode (3rd Order) shape (18.502 Hz) based on numerical analysis (Abaqus).

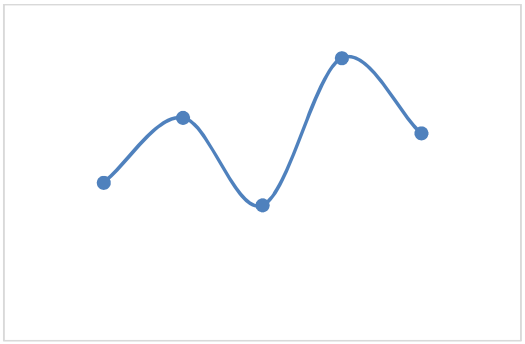

Figure 20b. Third Mode (3rd Order) shape (18.555 Hz) based on modal testing (Experimental).

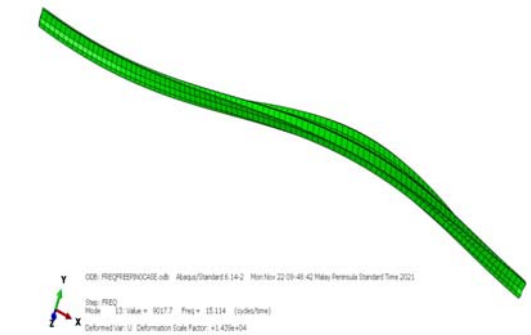

Figure 21a. Fourth Mode (4th Order) shape (15.114 Hz) based on numerical analysis (Abaqus).

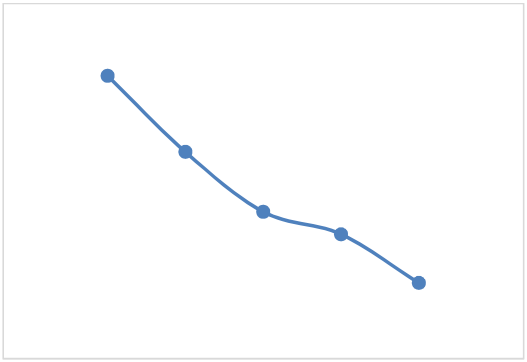

Figure 21b. Fourth Mode (4th Order) shape (15.137 Hz) based on modal testing (Experimental).

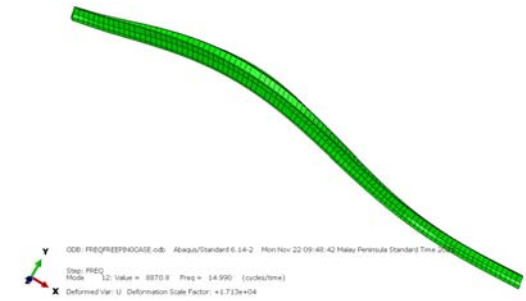

Figure 22a. Fifth Mode (5th Order) shape (14.990 Hz) based on numerical analysis (Abaqus).

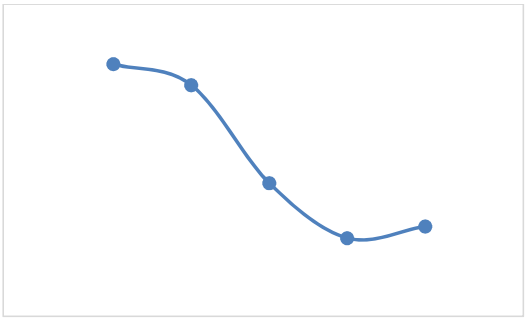

Figure 22b. Fifth Mode (5th Order) shape (14.893 Hz) based on modal testing (Experimental).

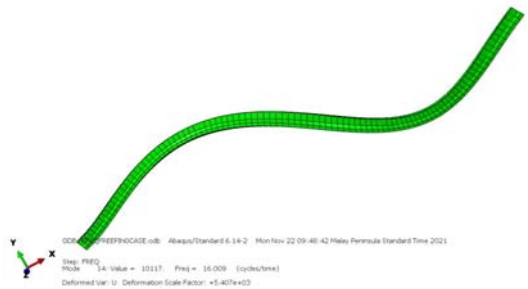

Figure 23a. Sixth Mode (6th Order) shape (16.009 Hz) based on numerical analysis (Abaqus).

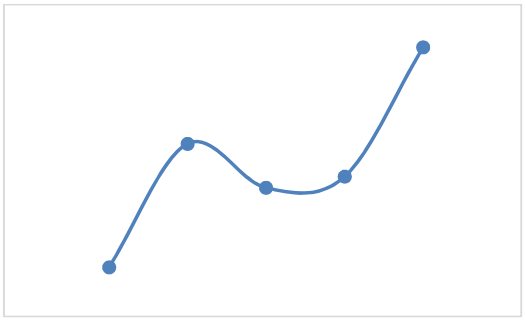

Figure 23b. Sixth Mode (6th Order) shape (16.357 Hz) based on modal testing (Experimental).

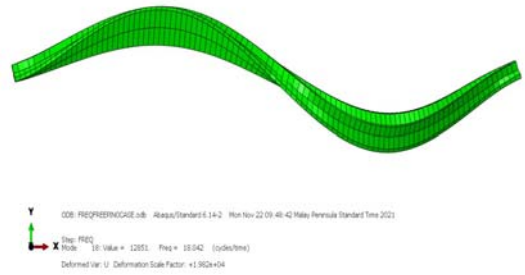

Figure 24a. Seventh Mode (7th Order) shape (18.042 Hz) based on numerical analysis (Abaqus).

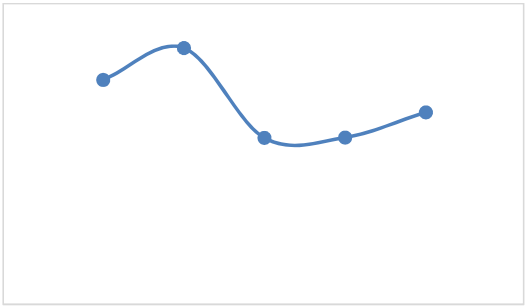

Figure 24b. Seventh Mode (7th Order) shape (18.311 Hz) based on modal testing (Experimental).

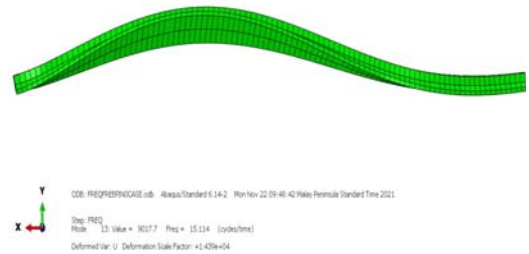

Figure 25a. Eighth Mode (8th Order) shape (15.114 Hz) based on numerical analysis (Abaqus).

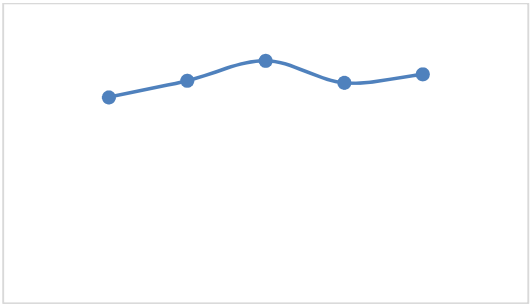

Figure 25b. Eighth Mode (8th Order) shape (15.137 Hz) based on modal testing (Experimental).

4.1.2 *Results of Experimental 2 (OMA).*

The difference between the vertical acceleration findings (see *Table 1*) obtained using the numerical approach (Abaqus result-output) and the field test (OMA test) was 8.94% mismatch or difference, which is less than the 15% limit that was set and targetted of this research study. This difference is attributed and classified as minor since it does not reach or exceed the limit. Therefore, this OMA test is acceptable for verification in numerical modelling results. Nevertheless, it is quite imperative to clarify the possibilities and reasons what the causes or factors that are contributing to this difference in percentage results. Among possibilities that are contributing to this difference: (1) Ambient or atmosphere temperature (humidity) factor does not consider in this modelling analysis which probably is giving slightly affects the concrete structure in terms of dynamic response where concrete structure does experience expansion and contraction in the daily cycle of movement. (2) Time dependant material factors such as creep strain, concrete elasticity and shrinkage strain in the concrete are not included in the numerical modelling stage which is considered to affect structural deformation (concrete shortening and bulging) due to permanent load (structure self-weight and prestressed force) which also affecting to the structural performance in resisting the loadings in the actual situation of bridge design life. The same goes for the result of Figure 26, these root-cause factors (temperature and time-dependent material) are also deemed to influence the structural response or acceleration [30][31] due to excitation loading(24-Tonnes truck). The pattern of acceleration response from both numerical and OMA test is visibly different due to the ambient or environment loading (wind/gust load) and time-dependent material factors were not included in numerical modelling. In addition to these, the exclusion of frequency of the truck itself [32], [33] in the numerical modelling could be driven-force to this acceleration difference as shown in figure 26. However, the acceleration of both results is lower than the allowable magnitude specified by codes such as Eurocode 2 and BS5400 which should be less than 0.7 m/s^2 [34][35][36][37]. Based on these two clues of result (Table 1 and Figure 26), this verification stage through the OMA test has indicated and proved that the numerical analysis results for modal properties analysis are acceptable and reliable state for structural dynamic investigation in this study.

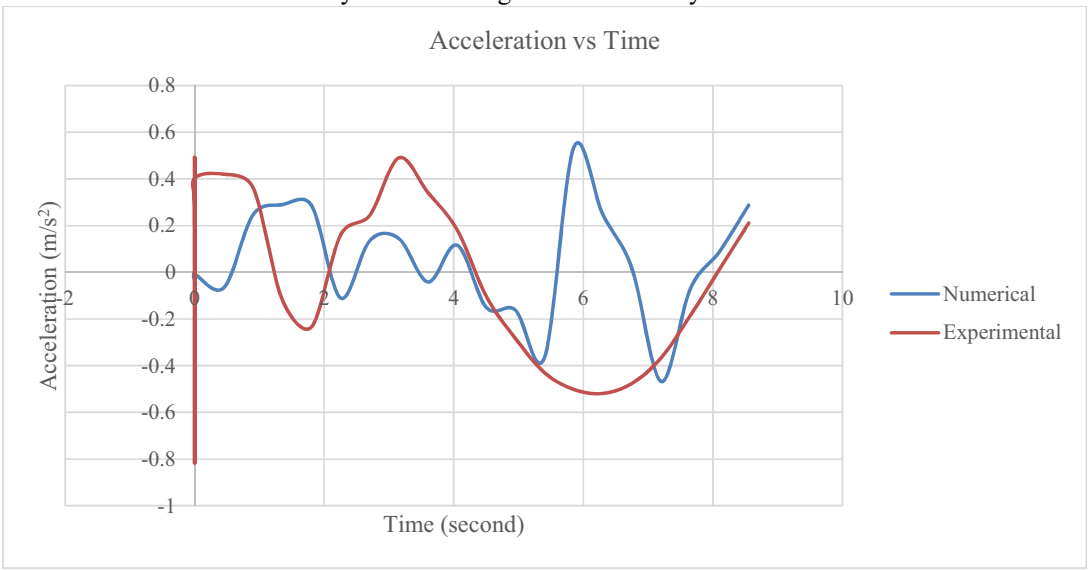

Figure 26. Comparison of accelerations between numerical and experimental.

Table 1. Results of accelerations between numerical and experimental.

Outputs	Experimental	Numerical	Error
Acceleration (m/s^2)	0.490	0.534	8.98 %

5.0 Conclusion

In this paper field test was carried out to evaluate the numerical analysis results, and the following conclusions can be drawn:

1. Generally, most natural frequency and mode shape results from EMA, the results are approximately similar to numerical results. However, some differences still exist in terms of frequency readings and mode shape results between the two methods of measurement because of some limitations such as external factors due to the existence of errors in both instruments (sensitivity value) and software (bugs) itself.
2. Based on EMA and numerical results, it can conclude that the first bending mode shape in terms of frequency value, the value shown in this bridge is not complying the minimum frequency requirement as stipulated in the BS code. The minimum frequency shall not be less than 5.0 Hz for the bridge to satisfy the dynamic requirements.
3. However, the acceleration reading both experimental and numerical shows that the current bridge acceleration is below the 0.7 m/s^2 acceleration limit based on the Eurocode limit.
4. From Table 1, the maximum acceleration values both OMA and numerical do not show a significant difference. The difference value between the above methods is less than 15 % which is meeting the boundary limit of this research.
5. To get better looks for mode shapes, it is recommended to add more detection points and response points which are constant interval spacings.
6. The method of fixing and mounting accelerometers and fibre optic cables shall be done securely and tightly so that they will not displace from their original position. This factor if not to be taken care could affect the data collection in terms of results consistency since both accelerometer and hammer are very sensitive devices in any surrounding movement.

Acknowledgement

The authors would like to send their warmest appreciation for the technical support from the School of Civil Engineering, Faculty of Engineering, Universiti Teknologi Malaysia and the financial research support from Universiti Teknologi Malaysia and Hanyang University Korea, No. R.J130000.7309.4B688. The author also would like thanks to Maju Expressway (MEX) Sdn. Bhd. and HSS Engineers Bhd. (HSS Integrated) for their support and assistance in this research.

References

[1] Y. Fujino and D. Siringoringo, "Vibration mechanisms and controls of long-span bridges: A review," *Struct. Eng. Int. J. Int. Assoc. Bridg. Struct. Eng.*, vol. 23, no. 3, pp. 248–268, 2013, doi: 10.2749/101686613X13439149156886.

[2] V. N. Dinh, K. Du Kim, and D. T. Hai, *Riding Comfort Assessment of High-Speed Trains Based on Vibration Analysis*, vol. 54, no. January. Springer Singapore, 2020.

[3] Y. Fujino, D. M. Siringoringo, Y. Ikeda, T. Nagayama, and T. Mizutani, "Research and Implementations of Structural Monitoring for Bridges and Buildings in Japan," *Engineering*,

vol. 5, no. 6, pp. 1093–1119, 2019, doi: 10.1016/j.eng.2019.09.006.
[4] Y. Fujino and D. M. Siringoringo, "Bridge monitoring in Japan: The needs and strategies," *Struct. Infrastruct. Eng.*, vol. 7, no. 7–8, pp. 597–611, 2011, doi: 10.1080/15732479.2010.498282.
[5] S. Chaiworawitkul, P. Omenzetter, and Y. Fujino, "Prediction of traffic-induced vibration using 3D bridge model and consideration of influence of bridge structural properties on response," *Proc. 2nd Int. Summer Symp. JSCE*, no. November 2014, 2000, doi: 10.13140/2.1.3406.4965.
[6] M. Tsubomoto, M. Kawatani, and K. Mori, "Traffic-induced vibration analysis of a steel girder bridge compared with a concrete bridge," *Steel Constr.*, vol. 8, no. 1, pp. 9–14, 2015, doi: 10.1002/stco.201510010.
[7] C. W. Kim, M. Kawatani, and W. S. Hwang, "Reduction of traffic-induced vibration of two-girder steel bridge seated on elastomeric bearings," *Eng. Struct.*, vol. 26, no. 14, pp. 2185–2195, 2004, doi: 10.1016/j.engstruct.2004.08.002.
[8] C. W. Kim, M. Kawatani, and K. B. Kim, "Three-dimensional dynamic analysis for bridge-vehicle interaction with roadway roughness," *Comput. Struct.*, vol. 83, no. 19–20, pp. 1627–1645, 2005, doi: 10.1016/j.compstruc.2004.12.004.
[9] M. I. Z. Ammar, E. Wahyuni, and D. Iranata, "Effects of Vibration Located on the Steel Truss Bridges under Moving Load," *IPTEK J. Proc. Ser.*, vol. 0, no. 1, p. 90, 2017, doi: 10.12962/j23546026.y2017i1.2198.
[10] B. Jeon, N. Kim, and S. Kim, "Estimation of the vibration serviceability deflection limit of a high-speed railway bridge considering the bridge-train interaction and travel speed Estimation of the Vibration Serviceability Deflection Limit of a High-speed Railway Bridge Considering the," no. May, 2015, doi: 10.1007/s12205-015-0565-z.
[11] S. Umar, N. Bakhary, and A. R. Z. Abidin, "Response surface methodology for damage detection using frequency and mode shape," *Meas. J. Int. Meas. Confed.*, vol. 115, no. October 2017, pp. 258–268, 2018, doi: 10.1016/j.measurement.2017.10.047.
[12] Y. B. Yang, C. W. Lin, and J. D. Yau, "Extracting bridge frequencies from the dynamic response of a passing vehicle," *J. Sound Vib.*, vol. 272, no. 3–5, pp. 471–493, 2004, doi: 10.1016/S0022-460X(03)00378-X.
[13] H. Excitations, A. Gheitasi, S. Usmani, M. Alipour, O. E. Ozbulut, and D. K. Harris, "Vibration Serviceability Assessment of an In-Service Pedestrian Bridge Under Vibration Serviceability Assessment of an In-Service Pedestrian Bridge Under Human-Induced Excitations," no. January, 2016, doi: 10.1007/978-3-319-29763-7.
[14] J. Yang, H. Ouyang, D. Stancioiu, S. Cao, and X. He, "Dynamic Responses of a Four-Span Continuous Plate Structure Subjected to Moving Cars With Time-Varying Speeds," *J. Vib. Acoust. Trans. ASME*, vol. 140, no. 6, pp. 1–15, 2018, doi: 10.1115/1.4039799.
[15] H. Dwairi, O. Al-Hattamleh, and H. Al-Qablan, "Evaluation of live-load distribution factors for high-performance prestressed concrete girder bridges," *Bridg. Struct.*, vol. 15, no. 1–2, pp. 15–26, 2019, doi: 10.3233/BRS-190149.
[16] W. Wang *et al.*, "The impact of traffic-induced bridge vibration on rapid repairing high-performance concrete for bridge deck pavement repairs," *Adv. Mater. Sci. Eng.*, vol. 2014, pp. 1–10, 2014, doi: 10.1155/2014/632051.
[17] O. S. Salawu and C. Williams, "Review of full-scale dynamic testing of bridge structures," *Eng. Struct.*, vol. 17, no. 2, pp. 113–121, 1995, doi: 10.1016/0141-0296(95)92642-L.
[18] P. Sen, "Sound principles," *Engineer*, vol. 291, no. 7606, p. 20, 2002, doi: 10.1119/1.2343605.
[19] O. S. Salawu and C. Williams, "Bridge Assessment Using Forced-Vibration Testing," *J. Struct. Eng.*, vol. 121, no. 2, pp. 161–173, 1995, doi: 10.1061/(asce)0733-9445(1995)121:2(161).
[20] P. Omenzetter *et al.*, "F Orced and a Mbient V Ibration T Esting," 2013.
[21] E. M. Rimmer, "The fundamentals of fastbus," *Interfaces Comput.*, vol. 3, no. 1, pp. 1–18, 1985, doi: 10.1016/0252-7308(85)90017-0.

[22] M. H. Richardson and D. L. Formenti, “Presented at 1,” pp. 1–15, 1982.
[23] M. H. Richardson, “Structural Dynamics Measurements - Rules of Digital Measurement,” pp. 1–13, 1999.
[24] R. Brincker, P. Andersen, and N. J. Jacobsen, “Automated frequency domain decomposition for operational modal analysis,” *Conf. Proc. Soc. Exp. Mech. Ser.*, 2007.
[25] L. Deng and C. S. Cai, “Identification of dynamic vehicular axle loads: Demonstration by a field study,” *JVC/Journal Vib. Control*, vol. 17, no. 2, pp. 183–195, 2011, doi: 10.1177/1077546309351222.
[26] J. D. Lindsey and J. T. Norris, “Study on the Effects of Excitation Characteristics in Operational Modal Analysis of Bridges,” *Transp. Res. Board 93rd Annu. Meet. January 12-16, Washington, D.C.*, no. July, pp. 1–15, 2014.
[27] M. Arjmand and W. Bratek, “Operational modal analysis to identify modal parameters in reciprocating compressors,” *GMRC Gas Mach. Conf.*, no. October, 2019.
[28] S. Cong, S. L. J. Hu, and H. J. Li, “FRF-based pole-zero method for finite element model updating,” *Mech. Syst. Signal Process.*, vol. 177, no. April, p. 109206, 2022, doi: 10.1016/j.ymssp.2022.109206.
[29] S. S. Saidin *et al.*, “Operational modal analysis and finite element model updating of ultra-high-performance concrete bridge based on ambient vibration test,” *Case Stud. Constr. Mater.*, vol. 16, no. May, p. e01117, 2022, doi: 10.1016/j.cscm.2022.e01117.
[30] A. Androus, H. M. Afefy, and K. Sennah, “Investigation of free vibration and ultimate behavior of composite twin-box girder bridges,” *J. Constr. Steel Res.*, vol. 130, pp. 177–192, 2017, doi: 10.1016/j.jcsr.2016.12.017.
[31] J. N. Mukabi, “Necessity to Review Resilient Properties and Resilient / Elastic Modulus Models of Pavement Materials for MEPD E-Publication Necessity for Review of Resilient Properties and Conventional Resilient Modulus Models of Characterizing Pavement Materials for ME,” no. October, pp. 1–28, 2016.
[32] D. Cantero, P. McGetrick, C. W. Kim, and E. OBrien, “Experimental monitoring of bridge frequency evolution during the passage of vehicles with different suspension properties,” *Eng. Struct.*, vol. 187, no. January, pp. 209–219, 2019, doi: 10.1016/j.engstruct.2019.02.065.
[33] Y. B. Yang *et al.*, “A novel frequency-free movable test vehicle for retrieving modal parameters of bridges: Theory and experiment,” *Mech. Syst. Signal Process.*, vol. 170, no. July 2021, 2022, doi: 10.1016/j.ymssp.2022.108854.
[34] K. Kasapova and D. Dinev, “HUMAN-INDUCED VIBRATIONS ON FOOTBRIDGES . CURRENT CODES OF PRACTICE -OVERVIEW,” no. February, 2020.
[35] K. Van Nimmen, G. Lombaert, G. De Roeck, and P. Van den Broeck, “Vibration serviceability of footbridges: Evaluation of the current codes of practice,” *Eng. Struct.*, vol. 59, pp. 448–461, 2014, doi: 10.1016/j.engstruct.2013.11.006.
[36] M. Mirteheri, “Ambient vibration testing of existing buildings : Experimental , numerical and code provisions,” vol. 10, no. 4, pp. 1–9, 2018, doi: 10.1177/1687814018772718.
[37] M. Mirtaheri and F. Salehi, “Ambient vibration testing of existing buildings: Experimental, numerical and code provisions,” *Adv. Mech. Eng.*, vol. 10, no. 4, pp. 1–9, 2018, doi: 10.1177/1687814018772718.